A Novel Lipid Hydroperoxide-Derived Modification to Arginine

ARTICLE *in* CHEMICAL RESEARCH IN TOXICOLOGY · JANUARY 2004

Impact Factor: 3.53 · DOI: 10.1021/tx034178l · Source: PubMed

A Novel Lipid Hydroperoxide-Derived Modification to Arginine

Tomoyuki Oe,[†] Seon Hwa Lee,[†] Maria V. Silva Elipe,[‡,§] Byron H. Arison,[‡] and Ian A. Blair*,[†]

Center for Cancer Pharmacology, University of Pennsylvania School of Medicine, 1254 BRB II/III, 421 Curie Boulevard, Philadelphia, Pennsylvania 19104-6160, and Department of Drug Metabolism, Merck Research Laboratories, P.O. Box 2000, Rahway, New Jersey 07065

Received August 27, 2003

The guanidine group present in the amino acid arginine was found to react with the lipid hydroperoxide-derived bifunctional electrophile, 4-oxo-2-nonenal. The reaction between N^{α}-*tert*-butoxycarbony-L-arginine and 4-oxo-2-nonenal resulted in the formation of an adduct (adduct A) that subsequently dehydrated on heating to adduct B. Liquid chromatography/mass spectrometry and nuclear magnetic resonance spectroscopy were used to assign the structure of adduct B as (N^{δ},$N^{\omega'}$-etheno-2′-heptanon-2″-one)-N^{α}-*t*-Boc-arginine. The reaction proceeded from initial reaction of the primary N^{ω}-amino group at the C-1 aldehyde of 4-oxo-2-nonenal. Subsequently, an intramolecular Michael addition of a secondary N^{δ}-amino group occurring at C-3 resulted in formation of the cyclic carbinolamine adduct A. Dehydration and rearrangement of the exocyclic imine resulted in the formation of adduct B, which contained a stable imidazole ring. The tetra peptide LRDE reacted with 4-oxo-2-nonenal primarily at arginine rather than at the amino terminus. This suggests that arginine-containing proteins can react with lipid hydroperoxide-derived 4-oxo-2-nonenal to form a novel imidazole modification.

Introduction

Lipid peroxidation of PUFAs,[1] which occurs during oxidative stress, is thought to play an important role in the development of degenerative diseases of aging such as cardiovascular disease and cancer (*1*−*3*). Lipid hydroperoxides are formed from PUFAs nonenzymatically by reactive oxygen species [superoxide (O_2^{-}), peroxide (O_2^{2-}), and hydroxyl radical ($HO^{\bullet}$)] or enzymatically by lipoxygenases and cyclooxygenases (*4*). Subsequent homolytic decomposition of the PUFA lipid hydroperoxides initiated by transition metal ions or vitamin C results in the formation of α,*β*-unsaturated aldehydic genotoxins, such as 4-oxo-2-nonenal, 4,5-epoxy-2(*E*)-decenal, and 4-hydroxy-2-nonenal (*5*, *6*). Among them, 4-oxo-2-nonenal is a particularly potent lipid hydroperoxide-derived bifunctional electrophile, which reacts with the DNA bases 2′-deoxyguanosine (dGuo) (*7*), 2′-deoxyadenosine (dAdo) (*8*, *9*), and 2′-deoxycytidine (dCyd) (*10*) to form heptanone−etheno adducts (Scheme 1).

Scheme 1. Reaction of dGuo, dAdo, and dCyd with 4-Oxo-2-nonenal[a]

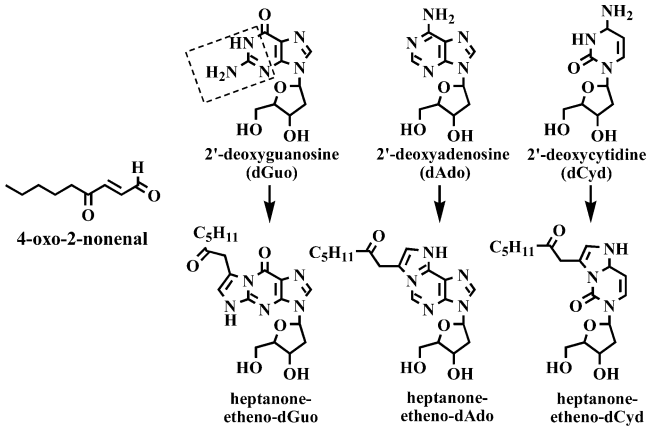

[a] The box shows the guanidine moiety that is also present in the amino acid arginine.

Several studies have demonstrated that 4-hydroxy-2-nonenal and other lipid hydroperoxide-derived bifunctional electrophiles can also induce covalent modifications with model amino acids and proteins (*11*−*17*). We speculated that the guanidine moiety present in the amino acid arginine would react with 4-oxo-2-nonenal to give stable adducts in an analogous manner to that observed with dGuo (Scheme 1; box). Therefore, covalent modifications to arginine could occur as a result of lipid peroxidation induced enzymatically or nonenzymatically during intracellular oxidative stress. The reaction between arginine derivatives and 4-oxo-2-nonenal has been reported by Doorn and Petersen (*18*, *19*). However, the structure of the arginine adduct was not determined. Arginine is an important amino acid that is found free

* To whom correspondence should be addressed. Fax: (215)573-9889. E-mail: ian@spirit.gcrc.upenn.edu.
[†] University of Pennsylvania School of Medicine.
[‡] Merck Research Laboratories.
[§] Current address: Amgen, Process Development−Analytical Sciences Department, 1 Amgen Center Drive (Mail Stop 30W-3-A), Thousand Oaks, CA 91320.

[1] Abbreviations: bd, broad doublet; *t*-Boc, tertiary butoxycarbonyl; bt, broad triplet; CID, collision-induced dissociation; COSY, ^{1}H,^{1}H-2D correlation spectroscopy; DMSO, dimethyl sulfoxide; ESI, electrospray ionization; HMBC, ^{1}H,^{13}C-2D heteronuclear multiple bond correlation; HSQC, ^{1}H,^{13}C-2D heteronuclear single quantum correlation; 13-HPODE, 13-hydroperoxy-[*S*-(*Z*,*E*)]-9,11-octadecadienoic acid; LC/MS, liquid chromatography/mass spectrometry; MALDI-TOF/MS, matrix-assisted laser desorption−ionization time-of-flight/mass spectrometry; MOPS, 3-(*N*-morpholino)propanesulfonic acid; MH^+, protonated molecular ion; MS^n, multiple tandem mass spectrometry; NMR, nuclear magnetic resonance; NOE, nuclear Overhauser effect; PUFAs, polyunsaturated fatty acids; ROESY, rotating frame nuclear Overhauser effect; PAD, photodiode array detector; TIC, total ion current.

10.1021/tx034178l CCC: $25.00
Published on Web 11/11/2003

in plasma as well as at the active site of many enzymes including nitric oxide synthase. Therefore, it is important to understand the precise nature of the chemical modification that has occurred on the arginine molecule. Here, we report the chemical structure of arginine modified with 4-oxo-2-nonenal using LC/ESI/MS and NMR spectroscopy. We also report the identification of the 4-oxo-2-nonenal-modified arginine in a model peptide.

Materials and Methods

Materials. N^{α}-*t*-Boc-L-Arginine hydrochloride, hydrogen fluoride, sodium borohydride, trifluoroacetic acid, nitric acid, ammonium hydroxide, and manganese dioxide were purchased from Sigma Chemical Co. (St. Louis, MO). Ammonium acetate was obtained from J. T. Baker (Phillipsburg, NJ). A model peptide, Leu-Arg-Asp-Glu (LRDE) was obtained from the Protein Chemistry Laboratory, University of Pennsylvania (Philadelphia, PA). MOPS was obtained from Fluka BioChemika (Milwaukee, WI). Chelex-100 chelating ion exchange resin (100−200 mesh size) was purchased from Bio-Rad Laboratories (Hercules, CA). HPLC grade water, acetonitrile, methanol, and methylene chloride were obtained from Fisher Scientific Co. (Fair Lawn, NJ). Ethanol was obtained from Pharmaco (Brookfield, CT). DMSO-d_6 was obtained from Sigma. Gases were supplied by BOC Gases (Lebanon, NJ).

NMR. The NMR spectra were determined at 25 °C using a 600 MHz for ^{1}H and 150 MHz for ^{13}C Varian Inova 600 instrument (Palo Alto, CA) equipped with a Nalorac 3 mm indirect detection gradient probe (Erfurt, Germany). Adduct B (ca. 2 mg) was dissolved in 150 μL of DMSO-d_6. Data processing was conducted directly on the NMR spectrometer. Chemical shifts are reported on the δ scale (ppm) by assigning the residual solvent peak to 2.49 and 39.5 ppm for DMSO for ^{1}H and ^{13}C, respectively. The ROESY experiment was determined with a 300 ms mixing time. The delay between successive pulses was 1 s for COSY and ROESY. Both the ^{1}H,^{13}C 2D HSQC and ^{1}H,^{13}C 2D HMBC spectra were determined using gradient pulses for coherence selection. The HSQC spectrum was determined with decoupling during acquisition. The delays corresponding to ^{13}C−^{1}H coupling ca. 140 Hz for the low pass filter and to ^{13}C−^{1}H long-range coupling constant of 7 Hz were used for the HMBC.

Mass Spectrometry. The data were acquired on a Finnigan LCQ ion trap mass spectrometer (Thermo Finnigan, San Jose, CA) equipped with a Finnigan ESI source. The mass spectrometer was operated in the positive ion mode with a potential of 4.5 kV applied to the electrospray needle. Nitrogen was used as the sheath (70 units) and auxiliary (5 units) gas to assist with nebulization. The capillary temperature was held at 200 °C. Full scanning analyses were performed in the range of *m*/*z* 150−750 (for N^{α}-*t*-Boc-L-arginine) or *m*/*z* 500−1000 (for LRDE). CID experiments coupled with MS^n employed helium as the collision gas. The relative collision energy for MS^n was set at 20−80% of the maximum (1 V).

Liquid Chromatography. Chromatography for LC/MS studies was performed using a Waters Alliance 2690 separation module (Waters Co., Milford, MA) equipped with an autosampler, vacuum degasser, column heater, and Hitachi L-4000 UV detector. Preparative LC was performed using a Hitachi L-7100 pump (Hitachi, San Jose, CA) with a Waters model 996 PAD and a Rheodyne model 7725 manual injector with a 500 μL sample loop (Rohnert Park, CA). System 1 employed a YMC ODS basic column (120 Å, 5 μm, 150 mm × 2.0 mm i.d.; Waters Co.). For system 1, solvent A was 5 mM aqueous ammonium acetate containing 0.01% (v/v) trifluoroacetic acid, and solvent B was 5 mM ammonium acetate in acetonitrile containing 0.01% (v/v) trifluoroacetic acid. The gradient for system 1 was as follows: 10% B at 0 min, 100% B at 18 min, 100% B at 20 min, 10% B at 21 min, and 10% B at 35 min with a flow rate of 0.25 mL/min. For a model peptide experiment, system 2 was performed using the same YMC ODS basic column used in system 1. For system 2, solvent A was 0.07% (v/v) trifluoroacetic acid in water, and solvent B was 0.07% (v/v) trifluoroacetic acid in acetonitrile. The gradient for system 2 was as follows: 1% B at 0 min, 91% B at 18 min, 91% B at 20 min, 1% B at 21 min, and 1% B at 40 min with a flow rate of 0.18 mL/min. System 3 employed YMC ODS-A column (120 Å, 5 μm, 150 mm × 4.6 mm i.d.) using isocratic elution with a mobile phase of acetonitrile/water (4:6, v/v; 0.5 mL/min). All separations were performed at ambient temperature.

Synthesis of 4-Oxo-2-nonenal. 4-Hydroxy-2-nonenal diethyl acetal was prepared from 4-hydroxy-2-nonynal diethyl acetal, which was reduced with lithium aluminum hydride. The product was oxidized with activated manganese dioxide as described by Esterbauer and Weger (*20*), and the resulting 4-oxo-2-nonenal diethyl acetal was hydrolyzed with citric acid/HCl as described previously (*7*).

Preparation of Metal Ion-Free Water. A slurry of 3.0 mL of hydrated Chelex-100 resin (ca. 200 mg dry weight) in the sodium form was packed into a borosilicate Pasteur pipet. The resin was washed with 15 mL of 2.5 M HNO_3 to elute any trace metal contamination. Excess acid was removed by washing the resin with 10 mL of water. The resin was transformed to the NH_4^+ form by the addition of 2.0 M NH_4OH (10 mL). Residual NH_4OH was removed from resin with 15 mL of water. The pH of the last few drops that eluted was checked with pH paper. HPLC grade water was then allowed to pass through the column, and the effluent was collected.

Preparation of Metal Ion Free-MOPS Buffer. Chelex-100 resin was treated in the same manner as the previous section. MOPS (2.157 g) was dissolved into ca. 80 mL of water. The solution was adjusted to pH 7 with 0.1 M HCl, followed by adding up to 100 mL in a volumetric flask. The buffer was then allowed to pass through the column, and the effluent was collected except for the first 10 mL. The buffer was kept in a polypropylene centrifuge tube to avoid further trace metal contamination from glassware.

Reaction of 4-Oxo-2-nonenal with N^{α}-*t*-Boc-L-Arginine Hydrochloride. A solution of 4-oxo-2-nonenal (154 μg, 1 μmol) in ethanol (20 μL) was added to N^{α}-*t*-Boc-L-arginine hydrochloride (1554 μg, 5 μmol) in Chelex-treated 100 mM MOPS buffer (pH 7, 200 μL). The reaction mixture was incubated at 37 °C for 24 h. A portion of the sample (20 μL) was analyzed by LC/MS using HPLC system 1.

Reaction of 4-Oxo-2-nonenal with N^{α}-*t*-Boc-L-Arginine Hydrochloride for MS^n Study. A solution of 4-oxo-2-nonenal (27.470 mg, 0.1781 mmol) in acetonitrile (1 mL) was added to N^{α}-*t*-Boc-L-arginine hydrochloride (17.392 mg, 0.056 mmol) in Chelex-treated water/acetonitrile (1:1, v/v; 2 mL). The reaction mixture was adjusted to pH 7 using 0.2 M NaOH prepared using Chelex-treated water and then incubated at 37 °C for 3 or 24 h. After the reaction, the solution was concentrated to half under N_2 stream and washed with ether (2 mL × 3). A portion of the sample (20 μL) was analyzed by LC/MS using system 1. The 3 h reaction mixture was then purified on system 3 following transformation and sodium borohydride experiments.

Transformation from Adduct A to Adduct B. A mixture of adduct A and adduct B (1:1) in water was heated at 80 °C for 4 h. A portion of the sample (20 μL) was analyzed by LC/MS using HPLC system 1.

Sodium Borohydride Reduction of Adduct A. Sodium borohydride (ca. 0.5 mg) was added to adduct A in water. The solution was kept at 4 °C for 15 min. A half of the solution was then incubated at 37 °C for 24 h. A portion of each sample (20 μL) was analyzed by LC/MS using HPLC system 1.

Synthesis of Adduct B for NMR Analysis. A solution of 4-oxo-2-nonenal (111.862 mg, 0.725 mmol) in acetonitrile (2 mL) was added to N^{α}-*t*-Boc-L-arginine hydrochloride (91.744 mg, 0.295 mmol) in Chelex-treated water/acetonitrile (1:1, v/v; 4 mL). The solution was adjusted to pH 7 with 1 M NaOH and then incubated at 37 °C for 24 h. After the reaction was complete, the solution was concentrated to 2 mL under a N_2 stream and washed with ether (2 mL × 3). The aqueous layer was semipurified with HPLC system 3 (t_R = 4.5−7 min) as a mixture of

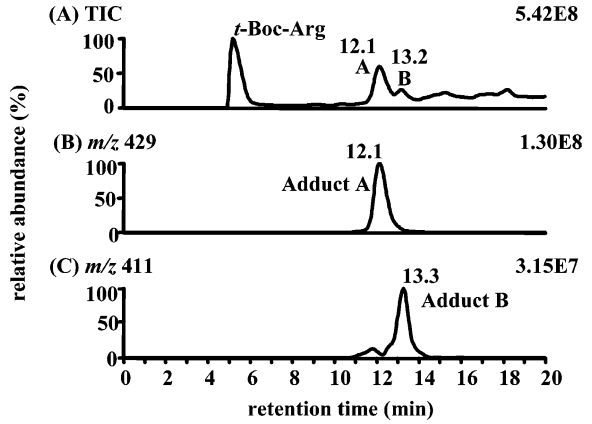

Figure 1. LC/MS analysis of adduct A and adduct B from the reaction of 4-oxo-2-nonenal with N^{α}-*t*-Boc-L-arginine. (A) TIC chromatogram. (B) The ion chromatogram for MH^+ of adduct A (*m*/*z* 429). (C) The ion chromatogram for MH^+ of adduct B (*m*/*z* 411).

adduct A and adduct B (almost 1:1). The crude fraction was heated at 80 °C for 4 h to complete the transformation to adduct B and then repurified twice by LC/PAD using HPLC system 3 (t_R = 5.1 min). Adduct B was obtained as a white amorphous powder (4.4 mg isolated, the reaction yield based on the recovered starting material was 21%) with purity >97% (UV λ_{max} 214.5 nm in 40% aqueous acetonitrile).

Deprotection of Adduct B. Aqueous hydrogen fluoride (48%, 1 μL) was added to adduct B (10 μg) in methylene chloride (100 μL). The solution was kept at room temperature for 1 h, concentrated to dryness under a N_2 stream, and redissolved into water (100 μL). A portion of the sample (20 μL) was analyzed by LC/MS using HPLC system 1.

Reaction of 4-Oxo-2-nonenal with LRDE for MS/MS Analysis. A solution of 4-oxo-2-nonenal (616 μg, 4.0 μmol) in ethanol (100 μL) was added to LRDE (426 μg, 0.8 μmol) in Chelex-treated 100 mM MOPS buffer (pH 7, 1000 μL). The reaction mixture was incubated at 37 °C for 13 or 36 h. Excess 4-oxo-2-nonenal was eliminated by ether extraction (1 mL × 3). A portion of the sample (20 μL) was analyzed by LC/MS using HPLC system 2.

Results

Reaction of 4-Oxo-2-nonenal with N^{α}-*t*-Boc-L-Arginine Hydrochloride. The reaction was performed using 4-oxo-2-nonenal with N^{α}-*t*-Boc-L-arginine hydrochloride in 100 mM MOPS buffer (pH 7) at 37 °C. The buffer was treated with Chelex-100 chelating ion exchange resin (*21*) to remove trace metal ions to prevent the formation of reactive oxygen species through Fenton reaction. LC/MS analysis revealed the presence of two major compounds with MH^+ ions at *m*/*z* 429 (t_R = 12.1 min, +154 Da; adduct A) and *m*/*z* 411 (t_R = 13.3 min, +136 Da; adduct B) on HPLC system 1 (Figure 1). Residual N^{α}-*t*-Boc-L-arginine (MH^+, *m*/*z* 275) was also observed at t_R = 4.5 min. At the initial stage of the reaction (3 h), the products were mainly adduct A. After 24 h, almost the same amounts of adduct A and adduct B were observed (1:1). With the LC/PD using HPLC system 3, adduct B showed a shift to higher λ_{max} (214.5 nm) than adduct A (<200 nm). This resulted from the formation of a conjugated double bond.

When a large excess of 4-oxo-2-nonenal was used, it was possible to detect byproducts, which consisted of one arginine and two 4-oxo-2-nonenals, by LC/MS. However, such a large excess of 4-oxo-2-nonenal is probably not physiologically relevant. Therefore, the byproducts were

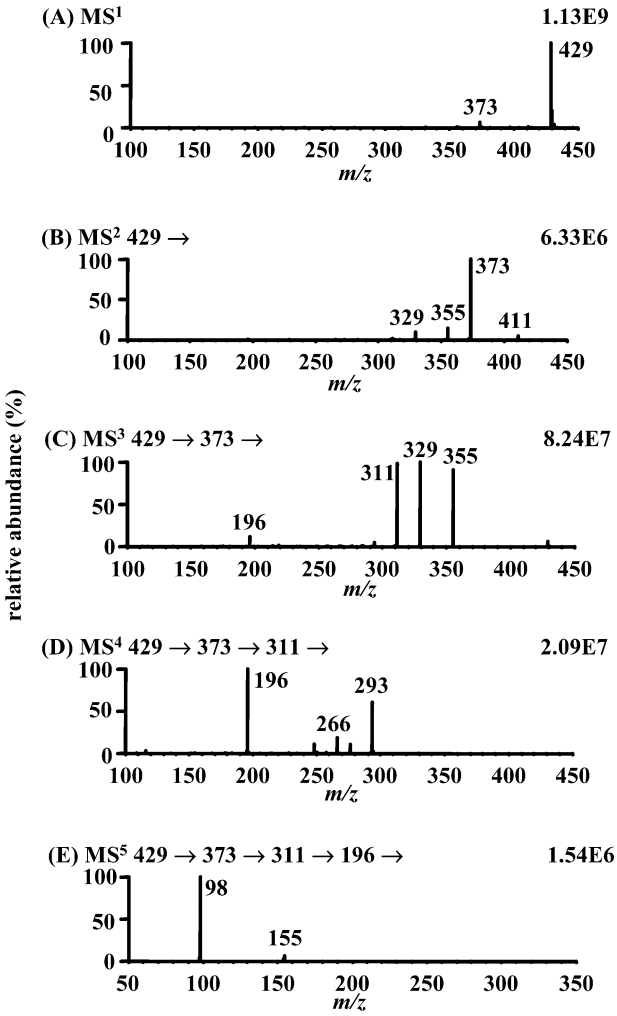

Figure 2. LC/MS^n analysis of adduct A. (A) Full scan mass (MS^1) spectrum, (B) MS^2 spectrum, (C) MS^3 spectrum, (D) MS^4 spectrum, and (E) MS^5 spectrum.

not fully characterized. In addition, there was no dramatic change in the rate of conversion of adduct A to adduct B when 10% ethanol or 67% acetonitrile was used. Although 10% ethanol is still nonphysiological, it represents a reasonable way to deliver such a hydrophobic molecule to an aqueous environment.

LC/MS^n Analysis of Adducts A and B. The mass spectrum of adduct A showed an intense MH^+ at *m*/*z* 429 with a minor fragment ion at *m*/*z* 373 ($MH^+ - t$-Bu + H) (Figure 2A). MS^2 analysis resulted in the formation of *m*/*z* 373 as a major product ion with the appearance of lower abundance ions at *m*/*z* 411 ($MH^+ - H_2O$), 355 ($MH^+ - t$-Bu $- H_2O$ + H), and 329 ($MH^+ - t$-Bu $- CO_2$ + H) (Figure 2B). MS^3 analysis revealed two additional ions at *m*/*z* 311 ($MH^+ - t$-Bu $- CO_2 - H_2O$ + H) and *m*/*z* 196 (protonated form of 2-amino-4-(heptane-2′-one)imidazole) (Figure 2C). This ion was more intense in the MS^4 spectrum (Figure 2D). Finally, the MS^5 spectrum showed an intense product ion at *m*/*z* 98 (2-methylimidazole + H) (Figure 2E). A similar series of product ions was observed in the mass spectrum of adduct B as compared with adduct A except for an ion at *m*/*z* 329 that resulted from a fragmentation pathway that did not involve dehydration (Figure 3A−E). MS^6 analysis was obtained for adduct B using the more sensitive infusion mode (Figure 3F). Three product ions (*m*/*z* 81, 71, and 56) were observed that resulted from the loss of NH_3 to form

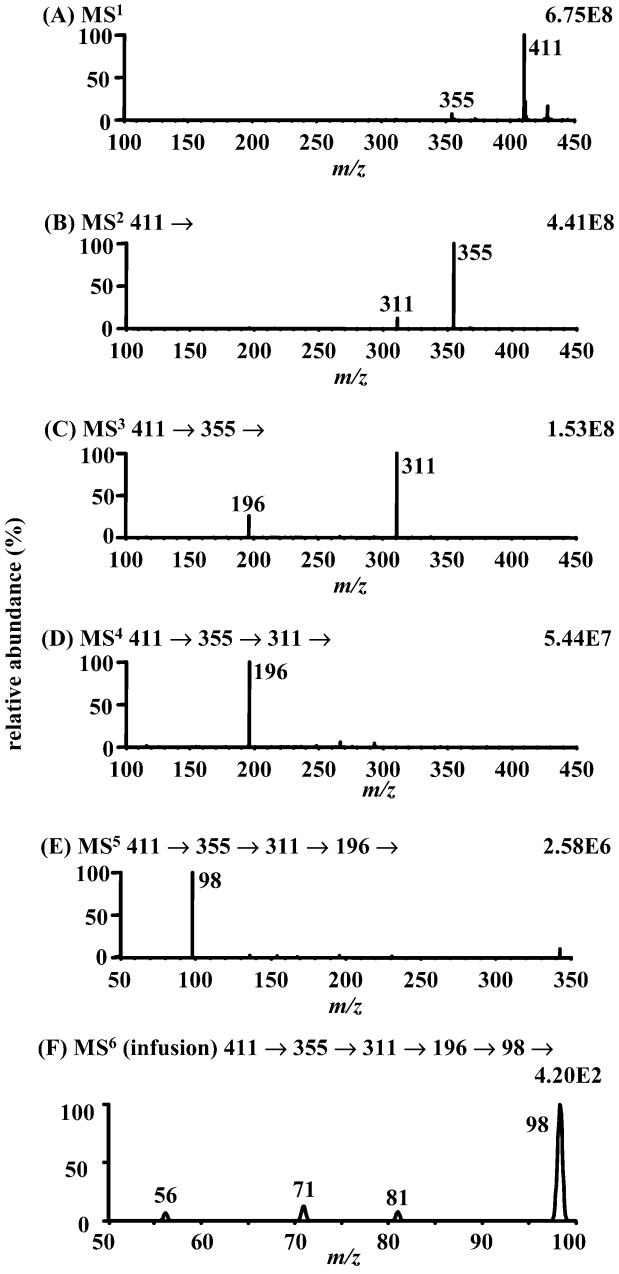

Figure 3. LC/MS^n analysis of adduct B. (A) Full scan mass (MS^1) spectrum, (B) MS^2 spectrum, (C) MS^3 spectrum, (D) MS^4 spectrum, (E) MS^5 spectrum, and (F) MS^6 spectrum.

4-methyl imidazole followed by ring cleavage as summarized in Scheme 2.

Transformation from Adduct A to Adduct B. A mixture of adduct A and adduct B (1:1) in water was heated at 80 °C. At the beginning of the reaction, the TIC showed adduct A and adduct B in similar amounts (Figure 4Aa). Reconstruction of MH^+ for adduct A revealed a significant signal (Figure 4Ab). Reconstruction of *m/z* 411 ($MH^+ - H_2O$ for adduct A and MH^+ for adduct B) revealed the expected two signals (Figure 4Ac). The LC/UV chromatogram (210 nm) showed a more intense signal for adduct B because of its UV chromophore (Figure 4Ad). After 4 h, the TIC showed essentially one major product (Figure 4Ba). The signal for MH^+ of adduct A in the channel corresponding to *m/z* 429 could barely be detected. Furthermore, adduct A was not detected in the channel corresponding to MH^+ of adduct B (*m/z* 411) or in the LC/UV chromatogram (Figure 4Bd).

Scheme 2. MS^n Fragmentation Pathways of Adduct B

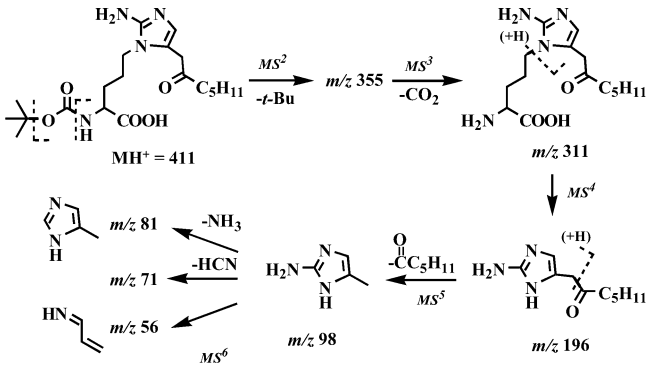

LC/MS^n Analysis of Adduct A after Sodium Borohydride Reduction. Adduct A was reduced by sodium borohydride. At the early stage of the reaction (at 4 °C for 15 min), the main product ($t_R = 10.3$) showed 2 mass unit-shifted MH^+ ions at *m/z* 431. MS^2 analysis of *m/z* 431 revealed a similar pattern of mass spectrum to that obtained adduct A except for a 2 mass unit shift, which suggested that the reduction occurred on the side chain carbonyl group. The reaction mixture was subsequently incubated at 37 °C for 24 h. The main product ($t_R = 10.4$ min) showed 4 mass unit-shifted MH^+ ion at *m/z* 433, resulting from reductions at both the carbonyl group and the imine group. MS^2 and subsequent MS^3 analyses of *m/z* 433 exhibited stepwise loss of *tert*-butyl and CO_2. MS^4 analysis of *m/z* 333 revealed product ions at *m/z* 288 and 176 corresponding to loss of CHO_2 and $C_9H_{17}O_2$, respectively. MS^5 analysis of *m/z* 288 showed a product ion at *m/z* 176, which suggested CHO_2 was a part of $C_9H_{17}O_2$ (Scheme 3).

MS/MS Analysis of Deprotected Adduct B. LC/MS analysis of adduct B after removal of the *t*-Boc protection group revealed the presence of an intense ion at *m/z* 311, which had been observed previously in the MS^3 spectrum of *t*-Boc-protected adduct B (Figure 3C). MS^2 analysis of *m/z* 311 showed an intense daughter ion at *m/z* 196 resulting from 2-amino-4-(heptane-2′-one)imidazole as had been observed in the *t*-Boc-protected adduct A (Figure 2D) and adduct B (Figure 3D).

NMR Analysis of Adduct B. The assignments of the proton signals (Table 1) and carbon signals (Table 2) were made on the basis of the proton chemical shifts and proton−proton couplings and COSY, HSQC, and HMBC correlations. All assignments refer to the structure in Figure 5. The presence of the only aromatic proton as a singlet at 6.52 ppm suggested that the chemical shift of this proton (H-1′) was in agreement of being on an imidazole moiety (Figure 5). The HSQC spectrum placed the chemical shift for C-1′ at 114.7 ppm, which was in the range of imidazole methine carbons. The COSY spectrum showed the connectivities of the side chain of arginine. The proton at C-2 in arginine (3.72 ppm) was coupled to the protons at C-3 (1.61 and 1.53 ppm), the protons at C-3 were coupled to the protons at C-4 (1.52 ppm), and the protons at C-4 were coupled to the protons at 3.60 ppm. The chemical shift of the methylene protons of arginine at C-5 (3.60 ppm) suggested that the δ-nitrogen should be a part of the imidazole moiety (Figure 5). The HSQC spectrum placed the chemical shift for C-5 at 41.1, which is typical for arginine C-5. The triplet at 2.50 ppm was assigned to the methylene protons at C-3″

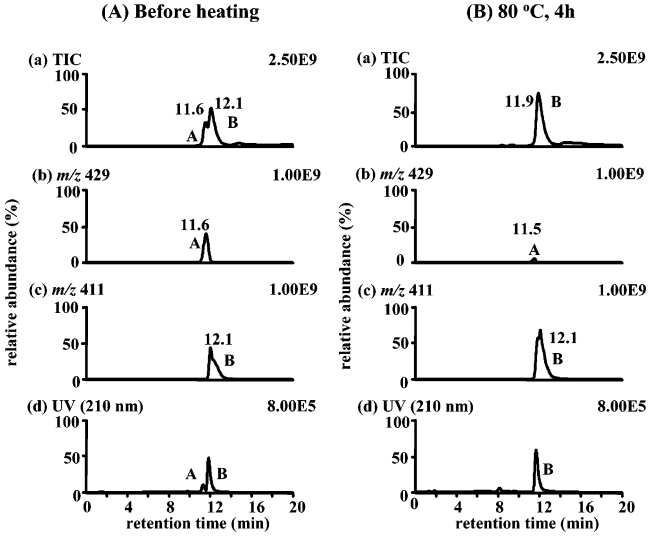

Figure 4. Analysis of the mixture of adduct A and adduct B. (A) Before heating (adduct A:adduct B = ca. 1:1) and (B) after heating at 80 °C for 4 h. (a) TIC chromatogram, (b) the ion chromatogram for MH^+ of adduct A (*m*/*z* 429), (c) the ion chromatogram for MH^+ of adduct B (*m*/*z* 411), and (d) UV chromatogram at 210 nm.

Scheme 3. Proposed Mechanism for Formation of Adduct A, Adduct B, and Reduction Products of Adduct A with $NaBH_4$

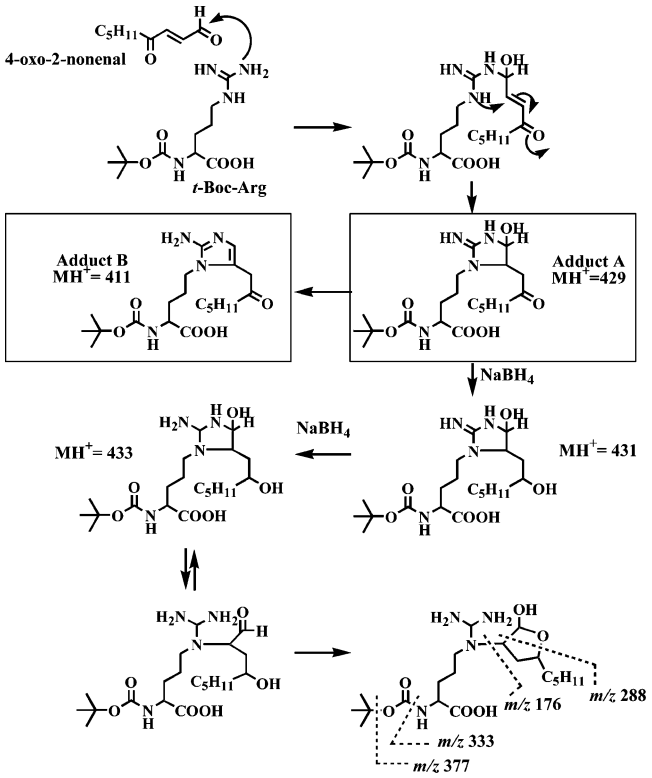

because of its chemical shift and its multiplicity (Figure 5). The COSY spectrum also showed the correlations between the C-3″ protons with the C-4″ protons (1.46 ppm), the C-4″ protons and the C-5″ protons (1.25 ppm), the C-5″ protons with the C-6″ protons (1.19 ppm), and, finally, the C-6″ protons with the methyl group at C-7″ (0.84 ppm). The ROESY experiment showed two NOE cross-peaks between the methylene protons at C-1″ (3.72 ppm) with the aromatic proton H-1′ (6.52 ppm) and this methylene (3.72 ppm) with the protons of the methylene of arginine at C-5 (3.60 ppm) (Figure 6), pointing out the

Table 1. ^{1}H NMR Assignments for Adduct B[a]

assigned H	δ (ppm)	multiplicities	H-coupled (J Hz)	type
H-1′	6.52	singlet		−C=C*H*
H-α	6.32	bd	H-2 (6.6)	−N*H*−CH
H-2	3.72	multiplet		−NH−C*H*
H-1″a,b	3.72	singlet		−C*H*$_2$−CO
H-5a,b	3.60	bt	H-4a (6.8), H-4b (6.8)	−C*H*$_2$−N
H-3″a,b	2.50	triplet	H-4″a (7.3), H-4″b (7.3)	−C*H*$_2$−CO
H-3b	1.61	multiplet		−C*H*$_2$−C
H-3a	1.53	multiplet		−C*H*$_2$−C
H-4a,b	1.52	multiplet		−C*H*$_2$−C
H-4″a,b	1.46	multiplet		−C*H*$_2$−C
t-Bu	1.36	singlet		−C(C*H*$_3$)$_3$
H-5″a,b	1.25	multiplet		−C*H*$_2$−C
H-6″a,b	1.19	multiplet		−C*H*$_2$−C
H-7″	0.84	triplet	H-6″a (7.2), H-6″b (7.2)	C*H*$_3$−C

[a] Spectra were obtained in DMSO-d_6.

Table 2. ^{13}C NMR Assignments for Adduct B[a]

assigned carbon	δ (ppm)	coupling	type
C-7″	13.5	H-5″, H-6″	−*C*H$_3$
C-5″	21.5	H-4″, H-6″, H-7″	−*C*H$_2$−
C-4″	22.4	H-3″, H-5″, H-6″	−*C*H$_2$−
C-4	24.6	H-2, H-3a,b, H-5	−*C*H$_2$−
t-Bu	27.9		−C(*C*H$_3$)
C-3	28.4	H-2, H-5	−*C*H$_2$−
C-6″	30.4	H-3″, H-4″, H-5″, H-7″	−*C*H$_2$−
C-1″	37.0		−*C*H$_2$−CO
C-3″	40.8	H-4″, H-6″	−*C*H$_2$−CO
C-5	41.1	H-3a,b	N−*C*H$_2$−
C-2	53.6	H-3a,b	N−*C*H−CO
t-Bu	77.5	*t*C(CH$_3$)$_3$	−*C*(CH$_3$)
C-1′	114.7	H-1″	−C=*C*H
C-2′	120.4	H-1′, H-1″, H-5	−*C*=CH
C-6	147.9	H-1′, H-5	N−*C*=N
C-1	175.2	H-2, H-3a,b	−*C*OOH
C-2″	206.8	H-1″, H-3″, H-4″	−C=*O*

[a] Spectra were obtained in DMSO-d_6.

structure of adduct B depicted in Figure 5. The HMBC showed C−H correlations between the protons of the methylene of arginine at C-5 (3.60 ppm) and the two aromatic quaternary carbons of the imidazole moiety at C-2′ and C-6 (120.4 and 147.9 ppm, respectively) (Figure 7), supporting the ROESY data that suggested the structure of this compound as (N^{δ},$N^{\omega'}$-etheno-2′-heptanon-2″-one)-N^{α}-*t*-Boc-arginine.

Reaction of 4-Oxo-2-nonenal with LRDE. 4-Oxo-2-nonenal was reacted with a peptide LRDE at 37 °C. L^{185}RDE^{188} is a peptide fragment from the digestion of human serum albumin with *Staphylococcus aureus* V8. This was used as a model peptide to determine whether this region of the albumin could be a site of lipid hydroperoxide-derived covalent modifications. The modified peptide could then potentially be used as a dosimeter of oxidative damage in vivo. LC/MS analysis of the reaction mixture using HPLC system 2 after 13 h revealed the presence of two major product peaks in the TIC (Figure 8Aa). Reconstruction of MH^+ (*m*/*z* 532) for the LRDE tetrapeptide showed that there was a significant amount of starting material still present (Figure 8Ab). The two major products were observed with MH^+ at *m*/*z* 668 (+136 Da) (t_R = 15.0 min, adduct 1; t_R = 15.8 min, adduct 2) (Figure 8Ac). They were also observed in the LC/UV chromatogram (Figure 8Ad). After 36 h, the only one major product was observed in the TIC (Figure 8Ba). There was still a substantial amount of starting

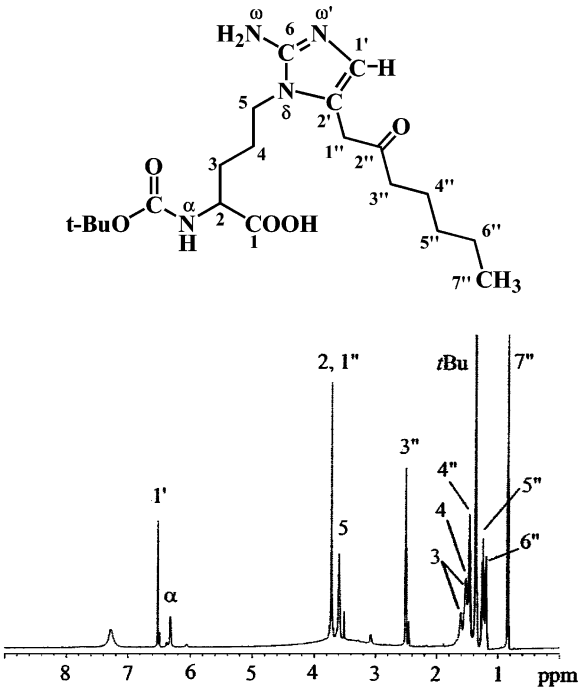

Figure 5. ^{1}H NMR spectrum of adduct B in DMSO-d_6. No signals were detected >9 ppm.

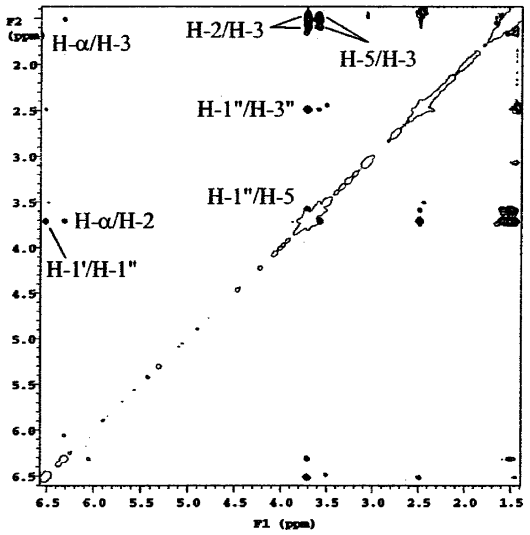

Figure 6. Expanded 2D ROESY spectrum of adduct B in DMSO-d_6.

compound present (Figure 8Bb). However, from the reconstructed ion corresponding to *m/z* 668 (Figure 8Bc) and the LC/UV chromatogram (Figure 8Bd), almost the entire product corresponded to adduct 2. The mass spectra for adduct 1 (Figure 9Aa) and adduct 2 (Figure 9Ba) were essentially identical. MS^2 analysis of adduct 1 clearly showed a modified b_1 ion at *m/z* 222.1 (*22*, *23*), which was consistent with an *N*-terminal modification, rather than an arginine modification (Figure 9Ab). However, adduct 2 showed a modified y_3 ion (*m/z* 555.2) and a modified b_2 ion (*m/z* 406.2) without a modified b_1 ion at *m/z* 222.1 (Figure 9Bb). This suggested that the modification had occurred on arginine rather than at the *N*-terminus.

Discussion

We have shown that 4-oxo-2-nonenal is one of the major products of lipid peroxidation (*5*) and that it forms

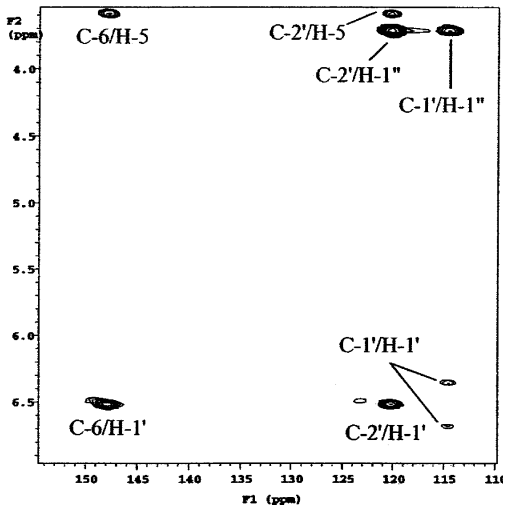

Figure 7. Expanded 2D ^{1}H,^{13}C HMBC spectrum of adduct B in DMSO-d_6.

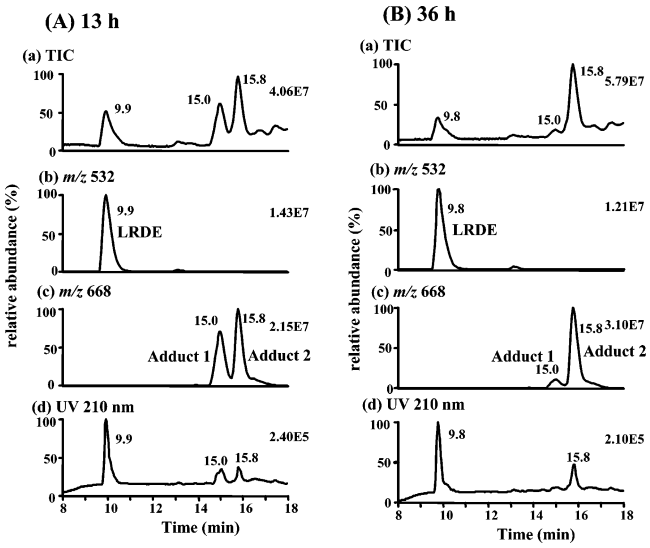

Figure 8. LC/MS analysis of the reaction between LRDE and 4-oxo-2-nonenal. (A) After reaction for 13 h. (B) After reaction for 36 h. (a) TIC chromatogram, (b) the ion chromatogram for MH$^+$ of LRDE (*m/z* 532), (c) the ion chromatogram for *m/z* 668, and (d) UV chromatogram at 210 nm.

adducts with dGuo (*7*), dAdo (*8*, *9*), and dCyd (*10*). A number of studies have demonstrated that 4-hydroxy-2-nonenal and its homologues can modify peptides and proteins (*11*−*15*, *17*). We realized that the guanidine moiety present in arginine could react with 4-oxo-2-nonenal in an analogous manner to that observed with dGuo (Scheme 1; box). Initial experiments were conducted with the *N*-terminal-protected arginine. The regioselectivity of the reaction with 4-oxo-2-nonenal was assigned with ROESY data obtained from the dehydrated stable product (adduct B). Two NOE cross-peaks were observed between the C-1″ methylene protons with the H-1′ aromatic proton and the C-1″ methylene protons with the C-5 methylene protons of arginine (Figure 5). This indicated that the intramolecular cyclization occurred on N^{δ}, not N^{ω} (Scheme 3). LC/MS data and labeling experiments conducted with sodium borohydride were consistent with this assignment.

In previous studies with dGuo, we have rationalized the high regioselectivity of the reaction with 4-oxo-2-nonenal results from initial attack of the primary amine

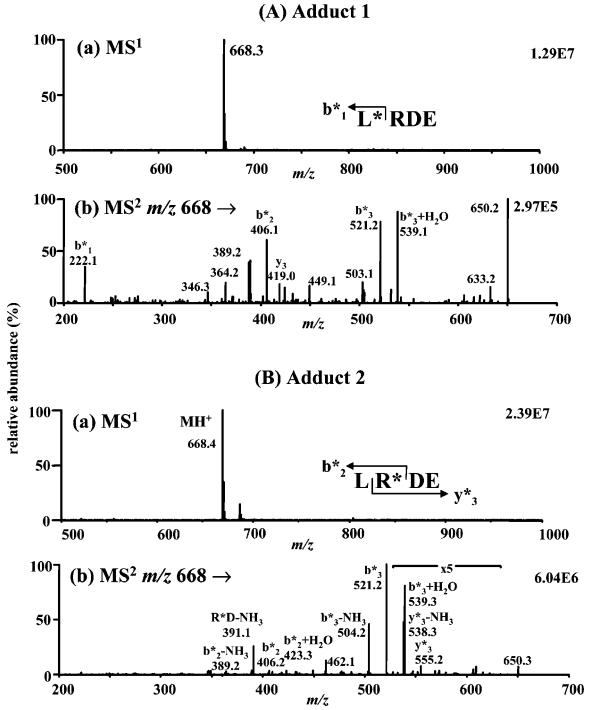

Figure 9. (A) LC/MS analysis of the LRDE adduct 1. (a) Full scan mass (MS^1) spectrum of adduct 1. (b) MS^2 spectrum of adduct 1 from *m/z* 668. (B) LC/MS analysis of LRDE adduct 2. (a) Full scan mass (MS^1) spectrum of adduct 2. (b) MS^2 spectrum of adduct 2 from *m/z* 668. The asterisk indicates that the product ion contains the modification (+136 Da).

of dGuo at the C-1 aldehyde (*7*). Therefore, we propose that a similar reaction occurs between 4-oxo-2-nonenal and *t*-Boc-arginine. Initial reaction of the primary N^{ω}-amino group occurs at C-1 of 4-oxo-2-nonenal and results in the formation of a carbinolamine intermediate (Scheme 3). An intramolecular Michael addition of the N^{δ} secondary amine to C-3 of the α,β-unsaturated ketone of the original 4-oxo-2-nonenal then occurs. This results in formation of a cyclic carbinolamine intermediate (adduct A) that is 154 Da higher in mass than *t*-Boc-arginine (Figure 3). Dehydration of adduct A and rearrangement of the exocyclic imine to a conjugated system results in the formation of the imidazole derivative (adduct B) 136 Da higher in mass than *t*-Boc-arginine (Figure 3). It is unlikely that 1,4-Michael addition precedes carbinolamine formation because the addition would occur preferentially at the more reactive α,β-unsaturated aldehyde rather than the α,β-unsaturated ketone (*24*), which would result in formation of a different regioisomer. This proposed mechanism is essentially identical to that described for reaction of 4-oxo-2-nonenal with dGuo if N^1 of dGuo is considered to be equivalent to N^{ω} of arginine. Rearrangement to an imidazole observed with the arginine adduct does not occur with dGuo because the imine at N^3 is constrained by conjugation. The dehydrated 4-oxo-2-nonenal−arginine adduct (adduct B) was quite stable once it had been isolated. Adduct A was less stable than adduct B and readily dehydrated on heating at pH 7 (Figure 4). N^{α}-Acetyl-L-lysine, N^{α}-acetyl-L-histidine, and N^{α}-acetyl-L-cysteine were found to form adducts with 4-oxo-2-nonenal (data not shown). N^{α}-Acetyl-L-lysine formed what appeared to be a Schiff base adduct, whereas N^{α}-Acetyl-L-histidine and N^{α}-acetyl-L-cysteine appeared to form primarily Michael addition adducts. However, the adducts were unstable and so full structural studies were not performed. Therefore, it is likely that the more stable 4-oxo-2-nonenal−arginine type B adduct will be detected as a modification to proteins in vivo.

The reaction between the 4-oxo-2-nonenal and the tetrapetide LRDE resulted in the formation of two major peaks with MH^+ of *m/z* 668 (+136 Da) at the initial stage of the reaction (13 h) (Figure 8Ac). Adduct 1, which disappeared on heating, was modified on the amino terminus, probably as a Schiff base. Adduct 2, which showed modified y_3 (*m/z* 555.2) and b_2 (*m/z* 406.2) ions without a modified b_1 ion (*m/z* 222.1) clearly possessed the same imidazole modification that was observed with *t*-Boc arginine. This raises the possibility that similar modifications could occur on protein arginine residues.

Doorn and Peterson have recently studied the 4-oxo-2-nonenal-mediated modifications to N^{α}-acetyl arginine-amide and arginine containing N^{α}-acetyl peptides (*18*, *19*). They presumed that the adducts formed in these reactions arose from Michael addition reactions because a 154 Da mass shift was observed. The arginine adducts observed in these previous studies may in fact be similar to the cyclic carbinolamine adduct A that we have identified rather than simple Michael addition products. Chemical modifications to arginine from other aldehydic bifunctional electrophiles such as glyoxal (*25*, *26*) and methylglyoxal (*25*, *27*) have been reported. Glyoxal is formed from oxidative degradation of glucose and lipid peroxidation (*28*), whereas methylglyoxal is formed by the nonenzymatic and enzymatic degradation of glyceraldehyde-3-phosphate and dihydroxyacetophosphate as well as in the metabolism of acetone and the catabolism of threonine (*28*). Arginine is the required substrate for nitric oxide synthases (*29*). It is noteworthy that methylated arginine derivatives have been detected in the circulation and that they are capable of inhibiting nitric oxide synthases (*30*). Arginine adducts derived from 4-oxo-2-nonenal and other lipid hydroperoxide-derived bifunctional electrophiles may also be endogenously produced enzyme inhibitors. Furthermore, the bifunctional electrophiles may be capable of modifying functionally important arginine residues in nitric oxide synthase enzymes. Studies are currently under way to explore these possibilities.

Acknowledgment. We thank the Protein Chemistry Laboratory, University of Pennsylvania, for synthesizing the peptide LRDE. We gratefully acknowledge the financial support from the National Institute of Health in the form of an RO-1 Grant to I.A.B. (CA95586). Partial support was awarded by the Abramson Cancer Center of the University of Pennsylvania and is funded, in part, under a grant with the Pennsylvania Department of Health. The Department specifically disclaims responsibility for any analyses, interpretations, or conclusions.

References

(1) Ames, B. N., Shigenaga, M. K., and Hagen, T. M. (1993) Oxidants, antioxidants, and the degenerative diseases of aging. *Proc. Natl. Acad. Sci. U.S.A.* **90**, 7915−7922.
(2) Marnett, L. J. (2000) Oxyradicals and DNA damage. *Carcinogenesis* **21**, 361−370.
(3) Lee, S. H., and Blair, I. A. (2001) Oxidative DNA damage and cardiovascular disease. *Trends Cardiovasc. Med.* **9**, 148−155.
(4) Blair, I. A. (2001) Lipid hydroperoxide-mediated DNA damage. *Exp. Gerantol.* **36**, 1473−1481.
(5) Lee, S. H., and Blair, I. A. (2000) Characterization of 4-oxo-2-nonenal as a novel product of lipid peroxidation. *Chem. Res. Toxicol.* **13**, 698−702.

(6) Lee, S. H., Oe, T., and Blair, I. A. (2001) Vitamin C-induced decomposition of lipid hydroperoxides to endogenous genotoxins. *Science* **292**, 2083−2086.
(7) Rindgen, D., Nakajima, M., Wehrli, S., Xu, K., and Blair, I. A. (1999) Covalent modifications to 2′-deoxyguanosine by 4-oxo-2-nonenal a novel product of lipid peroxidation. *Chem. Res. Toxicol.* **12**, 1195−1204.
(8) Rindgen, D., Lee, S. H., Nakajima, M., and Blair, I. A. (2000) Formation of a substituted 1,N^6-etheno-2′-deoxyadenosine adduct by lipid hydroperoxide-mediated generation of 4-oxo-2-nonenal. *Chem. Res. Toxicol.* **13**, 846−852.
(9) Lee, S. H., Rindgen, D., Bible, R. A., Hajdu, E., and Blair, I. A. (2000) Characterization of 2′-deoxyadenosine adducts derived from 4-oxo-2-nonenal, a novel product of lipid peroxidation. *Chem. Res. Toxicol.* **13**, 565−574.
(10) Pollack, M., Oe, T., Lee, S. H., Silva Elipe, M. V., Arison, B. H., and Blair, I. A. (2003) Characterization of 2′-Deoxycytidine Adducts Derived from 4-Oxo-2-nonenal, a Novel Lipid Peroxidation Product. *Chem. Res. Toxicol.* **16**, 893−900.
(11) Sayre, L. M., Arora, P. K., Iyer, R. S., and Salomon, R. (1993) Pyrrole formation from 4-hydroxynonenal and primary amines. *Chem. Res. Toxicol.* **6**, 19−22.
(12) Friguet, B., Stadtman, E. R., and Szweda, L. I. (1994) Modification of glucose-6-phosphate dehydrogenase by 4-hydroxy-2-nonenal. *J. Biol. Chem.* **269**, 21639−21643.
(13) Cohn, J. A., Tsai, L., Friguet, B., and Szweda, L. I. (1996) Chemical characterization of protein-4-hydroxy-2-nonenal cross-link: Immunochemical detection in mitochondria exposed to oxidative stress. *Arch. Biochem. Biophys.* **328**, 158−164.
(14) Xu, G., and Sayre, L. M. (1998) Structural characterization of a 4-hydroxy-2-alkenal-derived fluorophore that contributes to lipoperoxidation-dependent protein cross-linking in aging and degenerative disease. *Chem. Res. Toxicol.* **11**, 247−251.
(15) Xu, G., Liu, Y., Kansal, M. M., and Sayre, L. M. (1999) Rapid cross-linking of proteins by 4-keto aldehydes and 4-hydroxy-2-alkenals does not arise from the lysine-derived monoalkylpyrroles. *Chem. Res. Toxicol.* **12**, 855−861.
(16) Salomon, R. G., Kaur, K., Podrez, E., Hoff, H. F., Krushinsky, A. V., and Sayre, L. M. (2000) HNE-derived 2-pentylpyrroles are generated during oxidation of LDL, are more prevalent in blood plasma from patients with renal disease or atherosclerosis, and are present in atherosclerotic plaques. *Chem. Res. Toxicol.* **13**, 557−564.
(17) Hashimoto, M., Sibata, T., Wasada, H., Toyokuni, S., and Uchida, K. (2003) Chemical and immunochemical characterization of configurational isomers of a 4-hydroxy-2-nonenal-histidine adduct. *J. Biol. Chem.* **278**, 5044−5051.
(18) Doorn, J. A., and Petersen, D. R. (2002) Covalent modification of amino acid nucleophiles by the lipid peroxidation products 4-hydroxy-2-nonenal and 4-oxo-2-nonenal. *Chem. Res. Toxicol.* **15**, 1445−1450.
(19) Doorn, J. A., and Petersen, D. R. (2003) Covalent adduction of nucleophilic amino acids by 4-hydroxynonenal and 4-oxononenal. *Chem.-Biol. Interact.* **143**−**144**, 93−100.
(20) Esterbauer, H., and Weger, W. (1967) Über die wirkungen von aldehyden auf gesunde und maligne zellen, 3. mitt.: synthese von homologen 4-hydroxy-2-alkenalen, II. *Monatsh. Chem.* **98**, 1994−2000.
(21) Buettner, G. R., and Jurkiewicz, B. A. (1996) Catalytic metals, ascorbate and free radicals: combinations to avoid. *Radiat. Res.* **145**, 532−541.
(22) Roepstorff, P., and Fohlman, J. (1984) Proposal for a common nomenclature for sequence ions in mass spectra of peptides. *Biomed. Mass Spectrom.* **11**, 601.
(23) Johnson, R. S., Martin, S. A., Biemann, K., Stults, J. T., and Watson, J. T. (1987) Novel fragmentation process of peptides by collision-induced decomposition in a tandem mass spectrometer: differentiation of leucine and isoleucine. *Anal. Chem.* **59**, 2621−2625.
(24) Zhang, W. H., Liu, J., Xu, G., Yuan, Q., and Sayre, L. M. (2003) Model Studies on Protein Side Chain Modification by 4-Oxo-2-nonenal. *Chem. Res. Toxicol.* **16**, 512−523.
(25) Lederer, M. O., and Klaiber, R. G. (1999) Cross-linking of proteins by Maillard process: Characterization and detection of lysine-arginine cross-links derived from glyoxal and methylglyoxal. *Bioorg. Med. Chem.* **7**, 2499−2507.
(26) Glomb, M. A., and Lang, G. (2001) Isolation and charecterization of glyoxal-arginine modifications. *J. Agric. Food Chem.* **49**, 1493−1501.
(27) Oya, T., Hattori, N., Mizuno, Y., Miyata, S., Maeda, S., Osawa, T., and Uchida, K. (1999) Methylglyoxal modification of protein. Chemical and immunochemical characterization of methylglyoxal-arginine adducts. *J. Biol. Chem.* **274**, 18492−18502.
(28) Thornalley, P. J. (1998) Glutathione-dependent detoxification of a-oxoaldehydes by the glyoxalase system: involvement in disease mechanisms and antiproliferative activity of glyoxalaase I inhibitors. *Chem.-Biol. Interact.* **111**−**112**, 137−151.
(29) Moncada, S., and Higgs, E. A. (1995) Molecular mechanisms and therapeutic strategies related to nitric oxide. *FASEB J.* **9**, 1319−1329.
(30) Tsikas, D., Boger, R. H., Sandmann, J., Bode-Berger, S. M., and Frolich, J. C. (2000) Endogenous nitric oxide synthase inhibitors are responsible for the L-arginine paradox. *FEBS Lett.* 1−3.

TX034178L